A. Bataille and T. Magnin†*

Comparison of the Surface Cracking Process in Uniaxial and Multiaxial Fatigue

REFERENCE Bataille, A. and Magnin, T., **Comparison of the Surface Cracking Process in Uniaxial and Multiaxial Fatigue**, *Multiaxial Fatigue and Design*, ESIS 21 (Edited by A. Pineau, G. Cailletaud and T. C. Lindley) 1996, Mechanical Engineering Publications, London, pp. 195–207.

ABSTRACT Uniaxial and multiaxial physical damage processes have been investigated on a medium carbon steel at room temperature in laboratory air. Surface damage accumulation has been described on a mesoscopic scale which is related to microstructural barriers. A classification of surface short cracks has been conducted on the basis of their surface length. High short-crack densities have been monitored. Torsion fatigue corresponds to the higher short-crack densities in low-cycle fatigue, typically 200 short cracks per mm^2. Two main shear directions are developed under torsion stressing. Sequential multiaxial fatigue has been investigated. The results show that a prior torsional fatigue is more detrimental than a prior push-pull fatigue. This has been related to first-sequence cracking modes and crack orientation.

1 Introduction

For several years low-cycle fatigue (LCF) has been investigated from a surface damage accumulation point of view (**1–5**). Under uniaxial loading LCF damage accumulates in the form of multiple short-crack developments. The lengths of the short cracks are comparable to that of the microstructure of the studied material for most of the fatigue life. The description of tension–compression fatigue has already been presented at a mesoscopic scale on a single-phase 316L stainless steel (**5–6**). The aim of this paper is to compare the fatigue damage process of a ferrite/pearlite material at the microstructural scale under tension–compression and torsion with the previous description. It is shown how torsion loading damage and tension–compression loading damage interact during cumulative damage. Cumulative damage reveals the basic importance of the first loading mode in the torsion to tension–compression sequence (or reverse) on the resulting residual lifetime.

2 Material and Experimental Details

The material is a medium carbon steel of composition (weight %) 0.45C, 0.93Mn, 0.26Si with yield, tensile strength and Young modulus of 500 MPa, 800 MPa

*Laboratoire de Structure et Propriétés de l'Etat Solide, URA CNRS 234, Batiment C6, Cité Scientifique - Université des Sciences et Technologies de Lille, F-59655 Villeneuve d'Ascq, Cedex, France.
†Ecole des Mines, Département Matériaux, 158 cours Fauriel, St Etienne, Cedex, France.

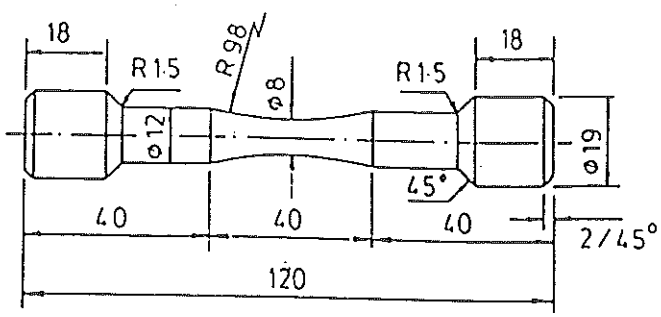

Fig 1 Ferrite/pearlite steel specimen shape for tension–compression fatigue and torsion fatigue.

and 210 GPa, respectively. The medium carbon steel microstructure is a typical normalized structure of a 0.45 wt%C steel where the ferrite phase in the form of rings has formed along the prior austenite grain boundaries. The isolated ferrite phase has a mean grain size of about 40 μm. The volume fraction of ferrite is approximately 30 percent, the remainder being pearlite.

Specimens with a mild hourglass profile have been used (Fig. 1). This shape limits the area of the cracking to the specimen centre in order to locate cracks around this point. After manufacture a stress relief treatment is conducted heating the specimens at 550°C for one hour followed by a slow cooling inside a furnace. Specimens are polished along the gauge length with emery papers down to grade 1200 followed by diamond pastes down to 1 μm finish. Specimen etching consists of a 45-second dip in 0.5% Nital and a 20-second dip in 4% Picral.

Replicas are taken for ten different stages in fatigue life. They are located from one stage to another referring to microhardness indentations in order to keep monitoring surface damage evolution of the chosen specimen centre area. Surface short-crack densities are determined on large areas in order to avoid local differences of LCF damage owing to local microstructural differences. Lifetimes are defined for both torsion and push-pull tests as the number of cycles (N_f) cumulated before the formation of a 1 mm length surface crack.

3 Tension–Compression Test Results

Fatigue tests have been performed at room temperature in laboratory air in fully reversed tension–compression loading on a servohydraulic fatigue testing machine.

A frequency of 1 Hz has been selected for low-cycle fatigue tests and a frequency of 5 Hz for high-cycle fatigue tests. Tension–compression tests with replication techniques have been conducted in load control at stress levels of $\Delta\sigma = 960$ MPa and $\Delta\sigma = 680$ MPa corresponding to lifetimes of approximately 7,000 cycles and 110,000 cycles, respectively. The cyclic tension–compression stress–strain equation in the power law strain-hardening region is given by

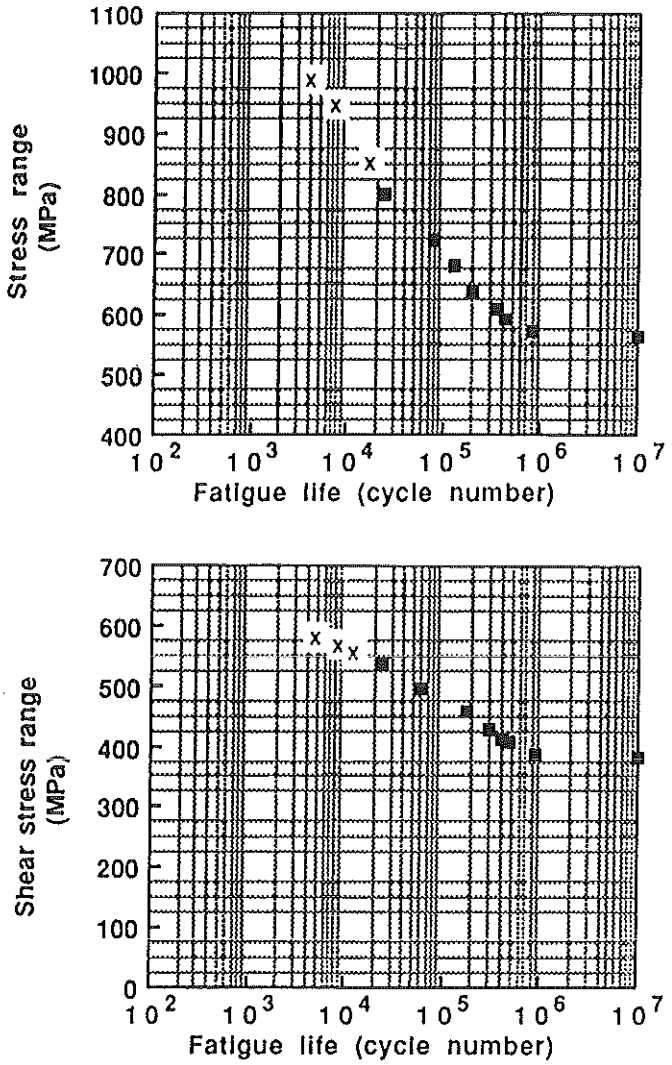

Fig 2 SN Curves: (a) tension–compression fatigue; (b) torsion fatigue (square symbols correspond to Zhang's experiments, cross symbols refer to Bataille's experiments).

$$\Delta\sigma = 2000(\Delta\varepsilon_p)^{0.2} \tag{1}$$

where $\Delta\sigma$ is expressed in MPa and $\Delta\varepsilon_p$ in m/m.

The fatigue endurance curve is shown in Fig. 2(a) (7, 8). As it has already been observed short cracks form at an early stage of the fatigue life, that is for less than 5% of (N_f) at all stress levels. The difference from one stress level to

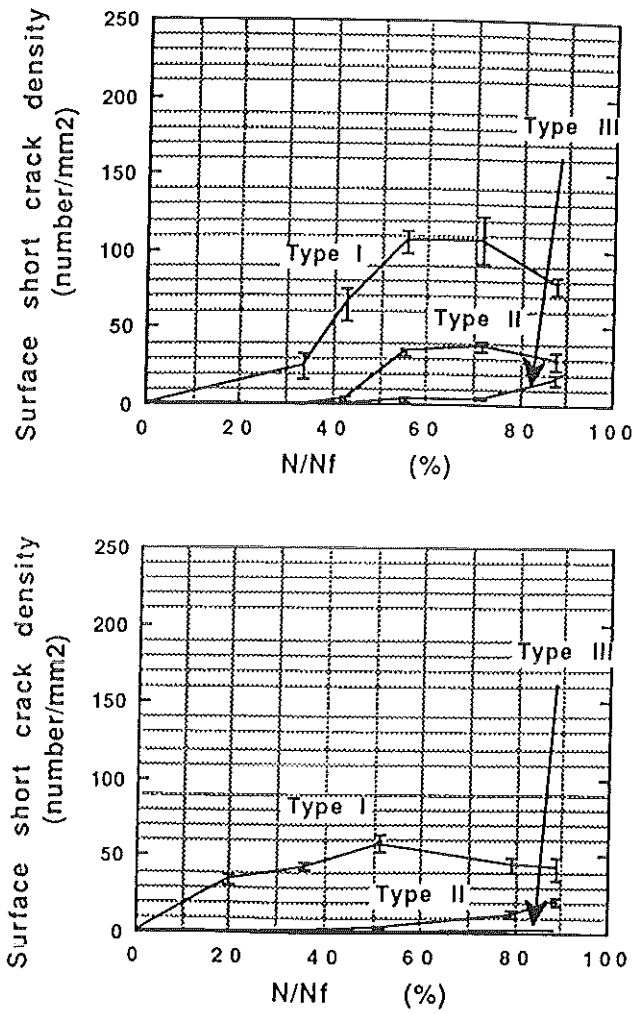

Fig 3 The developments of experimental surface short cracks in a specimen under tension–compression fatigue: (a) $\Delta\sigma = 960$ MPa, lifetime = 7000 cycles; (b) $\Delta\sigma = 680$ MPa, lifetime = 110 000 cycles.

another lies in the short-crack growth rates and the interactions between growing short cracks and the nature of the microstructure ahead of the crack tips.

Surface short cracks have been classified according to their surface length and to their growth behaviour. Type I short cracks correspond to those less than 40 to 50 microns at the surface (note this corresponds to the mean ferrite phase extension). Short cracks initiate in ferrite phase and show a steady growth as long as they are not near a transverse ferrite/pearlite interface. The latter interface strongly influences Type I short crack behaviour. Many Type I short

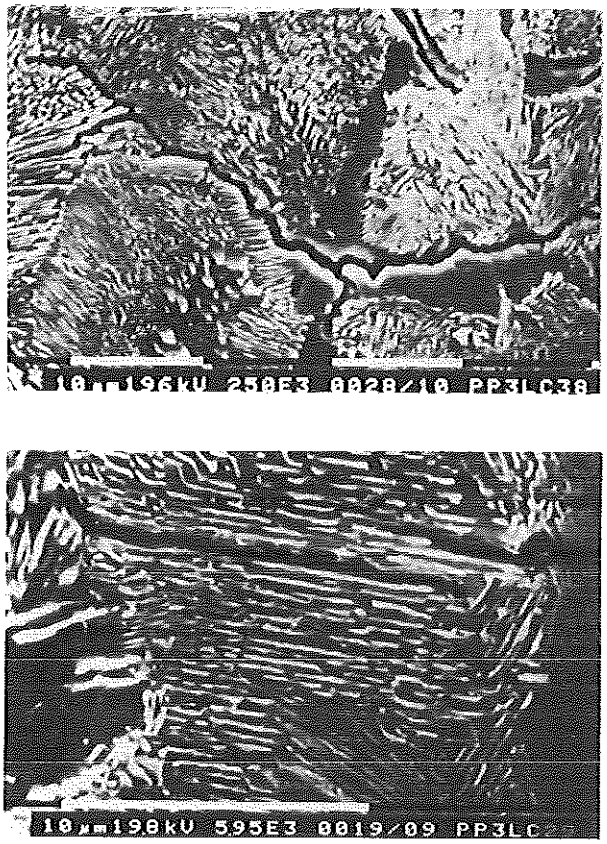

Fig 4 The short crack changes direction owing to local pearlite lamellae orientation (push–pull fatigue at $\Delta\sigma = 960$ MPa).

cracks are stopped at the ferrite/pearlite interfaces. However some of them overcome these microstructural barriers.

The second short crack type corresponds to those cracks having overcome 2 to 3 interfaces. The higher is the fatigue life the stronger is the influence of the interface on the crack development.

Type II cracks surface lengths range from 50 to 140–150 μm. Their growth undergoes little influence of the microstructure. Type III corresponds to short cracks longer than 150 microns. The monitoring of these three short-crack type populations at different stages in low-cycle fatigue reveals high crack densities at the surface (see Fig. 3 for surface short crack densities). The effect of the individual ferrite/pearlite interfaces on surface short crack development is small and a continuum mechanics representation may be employed (LEFM and EPFM behaviours).

Type I short crack corresponds to stage I and the growth mode is typically by shear in the ferrite phase where cracks initiate. The changeover from stage I to stage II takes place somehow during the crossing of 2 to 3 interfaces owing to the different local arrangements of pearlite lamellae orientation (Fig. 4).

All together short-crack densities reach 100 per mm^2 for a fatigue life of $N_f = 7000$ cycles and 60 per mm^2 for $N_f = 110000$ cycles. Many of those surface cracks are unable to overcome any barriers on their development paths and they are stopped near a microstructural barrier. However numerous short cracks reach the Type II range and propagate further.

Type II short-crack population strongly decreases, along with Type III, with stress level (from 40 per mm^2 at $\Delta\sigma = 960$ MPa to 10 per mm^2 at $\Delta\sigma = 680$ MPa, for a reduced lifetime of 40%). Furthermore the type II short-crack population exhibits a decrease corresponding to the formation of numerous Type III short cracks at $\Delta\sigma = 960$ MPa.

Such a decrease is observed also for Type I population. This must be associated with multiple interactions and hence coalescences between Type I and Type II short cracks at this stress level, once the Type I short-crack density has reached something like 100 per mm^2.

A steady state is observed in Type I populations from some 50% of reduced life to 75%. This may be explained by a nucleation rate of Type I surface short cracks equivalent to the rate of Type I population decrease to the benefit of upper short-crack densities. This steady state cannot be observed at $\Delta\sigma = 680$ MPa and the absence of a final decrease in Type I and Type II populations suggests that the formation of the fatal crack must be due to single-crack through-the-bulk propagation. Interestingly only a few Type III short cracks are found at the end of the test.

4 Reversed Torsion Results

Fatigue tests have been performed at room temperature in laboratory air in fully reversed torsion loading on an in-house built torsion rig. Torsion tests have been conducted in shear stress control at levels of $\Delta\tau = 580$ MPa and $\Delta\tau = 380$ MPa. Torsion fatigue lifetimes corresponded respectively to 7500 cycles and to 850000 cycles. The cyclic torsion stress–strain equation in the plastic region is given by:

$$\Delta\tau = 1300(\Delta\gamma_p)^{0.2} \tag{2}$$

where $\Delta\tau$ is expressed in MPa and $\Delta\gamma_p$ in m/m. A fatigue endurance curve is presented in Fig. 2(b) (7, 8).

Two main shear orientations exist in torsion: the lengthwise one and the transverse one. Fatigue damage accumulates through shear cracking along these directions. Figure 5 shows the evolution of the three above-defined categories of short-crack populations in torsion test for low-cycle fatigue (a) and high-cycle fatigue (b). At a stress level of $\Delta\tau = 580$ MPa the fatigue lifetime is comparable

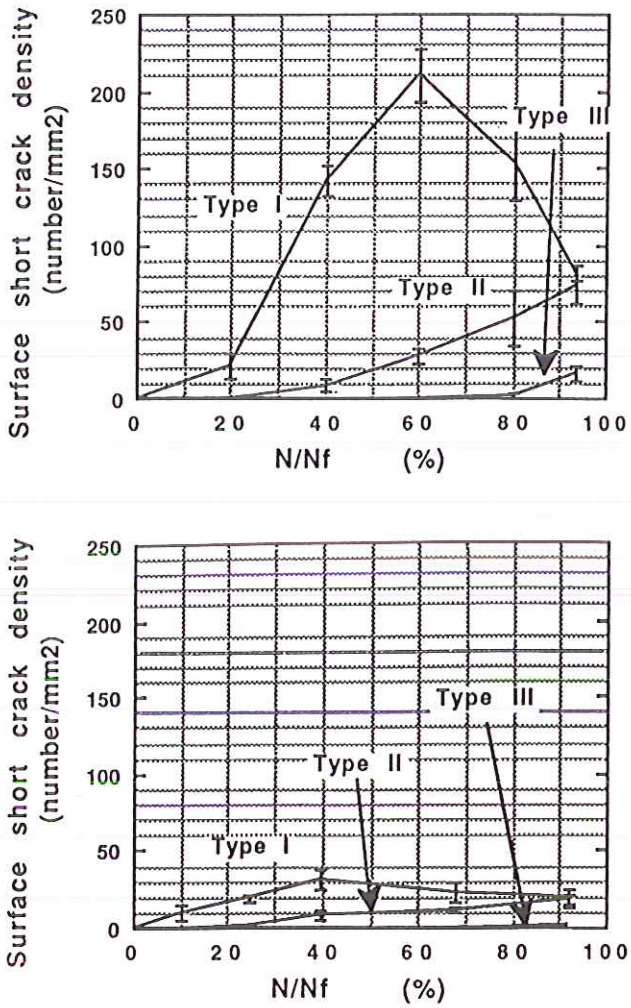

Fig 5 The d velopments of experimental surface short cracks in a specimen under torsion fatigue: (a) $\Delta\tau = 580$ MPa, lifetime = 7500 cycles; (b) $\Delta\tau = 380$ MPa, lifetime = 850 000 cycles.

to that in tension–compression at $\Delta\sigma = 960$ MPa. Some cracks are initiated very early in both main shear directions. Twenty percent of the reduced lifetime cracks are completed when an important evolution in the short-crack populations takes place. At 60 percent of reduced lifetime the higher Type I short-crack density is reached and some Type III short cracks form thereafter. Then Type I short-crack density decreases sharply corresponding to the quick formation of type III short cracks. The scatter in short-crack density measurement is far

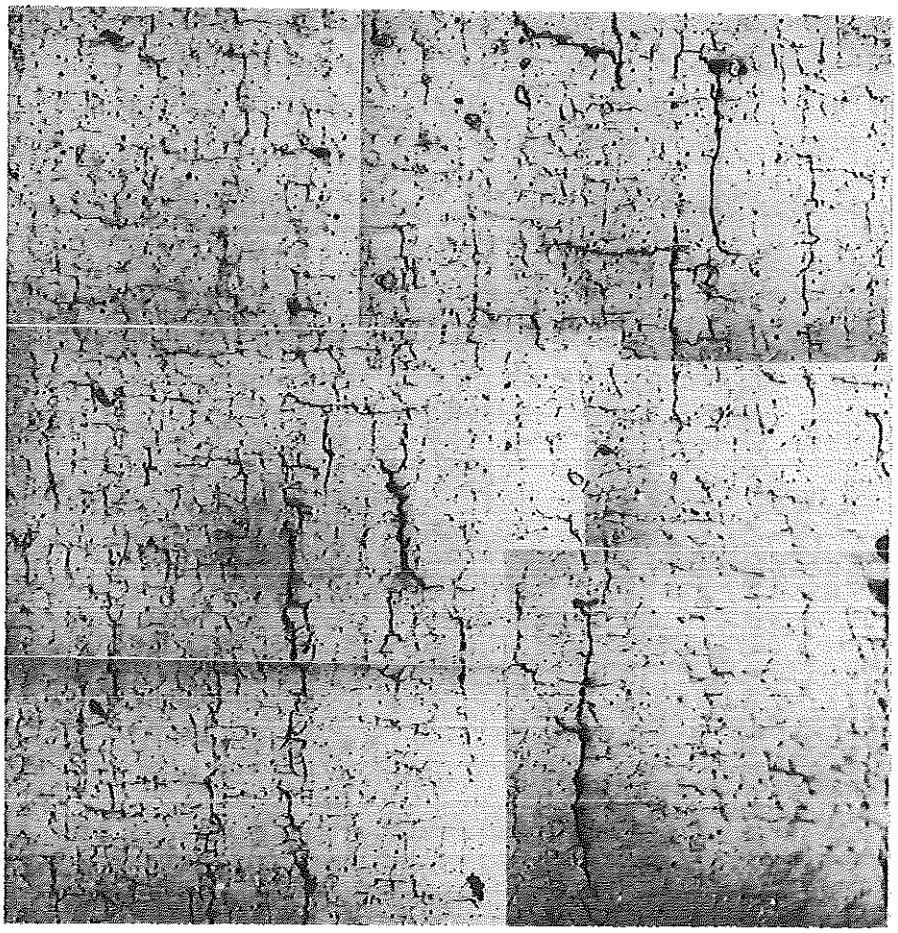

Fig 6 The specimen surface reveals high damage after completion of 6500 cycles under torsion at $\Delta\tau = 580$ MPa (specimen axis is vertical).

higher than for push-pull tests and no significant decrease of Type II population has been monitored.

Figure 6 shows a photograph of the specimen surface following completion of 6500 cycles out of a lifetime of 7500 cycles at the stree level of $\Delta\tau =$ 580 MPa. This photograph illustrates the high short-crack density reached and the intricate developments of short-cracks at the specimen surface. Hence it accounts most surely for multiple-resulting crack–crack interactions.

Such a high surface crack density has rarely been reported. Results presented elsewhere (8) show very clearly that the formation of the fatal crack results from multiple coalescences between surface short cracks. The maximum crack

densities in torsion are obtained for shorter reduced lifetimes compared to tension–compression tests.

In low-cycle fatigue there is little direction change during crack propagation due to intense shear stresses. However in high cycle fatigue some cracks change direction (rotation or branching) owing to ferrite/pearlite interface interactions. On branching or rotation the cracks tend to develop in a 45° direction with reference to the specimen axis. Changing direction corresponds also to a change in the cracking mode (from shear or mode III to tensile or mode I). Hence those new branches tend to develop naturally for lowest short-crack densities, that is at lowest shear stress levels. Such cracks exhibit a cruciform surface shape.

5 Discussion

5.1 *Comparison of tension–compression and torsion tests on the medium carbon steel*

Note that in the following, the results are compared for the same life. Short crack densities at specimen surfaces are much higher in torsion fatigue than in push-pull fatigue. They are twice as numerous on average. In low-cycle torsion fatigue crack–crack interactions result in shearing coalescence, the shear direction being in coincidence with the short crack growth direction.

Significant final decreases of the Type I and Type II short-crack densities are noted in low-cycle tension–compression fatigue. In torsion fatigue the final sharp decrease in Type I density suggests a more active role of Type I short cracks in the evolution of fatigue damage. The collective growth seems to extend on a larger lifetime range in torsion fatigue than in tension–compression fatigue since the crack densities remain high at the specimen surface even in the high-cycle fatigue regime. Some authors (**3**) suggested an easier coalescence occurrence in torsion than in push-pull. This may now be related to more favourable coalescence conditions due to the higher densities.

The aspect ratio is defined as the crack surface length over the crack depth. An important difference between a torsion short crack and a push-pull short crack lies in the aspect ratio. In tension–compression cracks tend to be half-penny shaped (**9**) whereas torsion fatigue short cracks are much more shallow. Though there is little literature about torsion crack aspects it is commonly admitted that the surface length approaches ten times the crack depth (**10**). This remark applies obviously to mode III cracking. Cruciform-shaped short cracks which form in high-cycle torsion fatigue are obviously different in their aspect.

An important microstructural feature has been pointed out: the ferrite/pearlite interface is the more effective microstructural obstacle to crack development. This is specially true for Type I and Type II short cracks.

5.2 *Comparison of low-cycle push-pull fatigue results in single-phase 316L stainless steel and in the medium carbon steel*

Push-pull fatigue of 316L alloy has been fully detailed previously in the literature

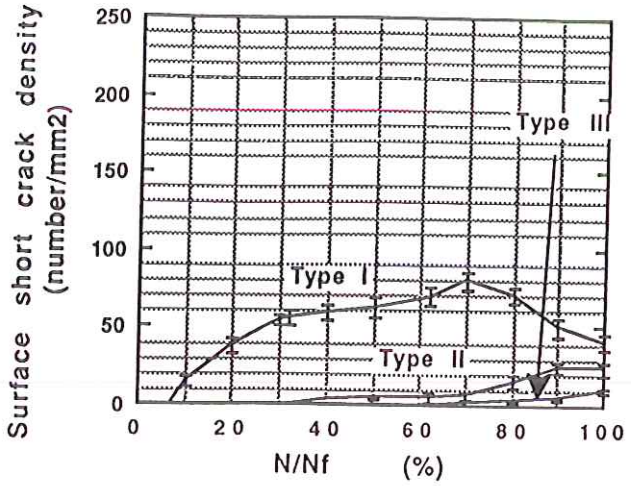

Fig 7 The development of experimental surface short cracks in a single-phase 316L stainless steel specimen under tension–compression fatigue, lifetime = 7000 cycles.

(5, 6, 8) and only the accumulation of surface fatigue damage will be considered below. The main crack development barrier in the single phase alloy was the grain boundary. The mean grain size was 50 μm. This led to a first classification of surface short cracks according to their surface length referred to the grain size. This classification has been extended to the medium carbon steel according to the mean distance between two important barriers to the crack surface propagation. Figure 7 presents the evolution of the short-crack population in low-cycle fatigue of 316L steel for a plastic strain-controlled experiment corresponding to a lifetime of 7500 cycles. The fatigue damage accumulates in the same way regardless of the nature of the alloy. The existence of several metallurgical phases simply changes the nature of the main crack propagation obstacle. This emphasizes the significant role of the short-crack density in the damage accumulation. The crack number results in a statistical aspect of the damage process. The statistics unify in this way the description of fatigue damage accumulation in low-cycle fatigue. The individual propagation of surface short cracks depends intimately of the microstructure of the studied alloys. Yet, as the crack number increases this is less and less true and the individual behaviour is replaced by a collective growth behaviour. The latter does not depend directly in itself on the microstructure.

6 Sequential Multiaxial Fatigue on Medium Carbon Steel

Cumulative damage has been investigated. Separate sequences of push-pull and of torsion were cumulated. The stress ranges have been chosen in order to obtain the same fatigue life when the specimen was subjected to one loading

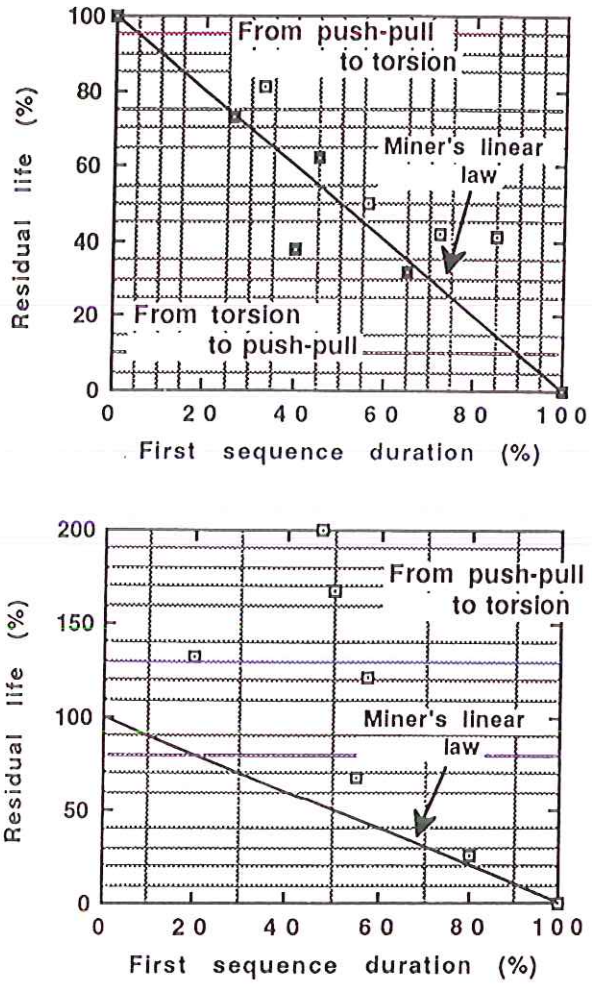

Fig 8 Sequential cumulative damage on medium carbon steel: (a) stress levels correspond to fatigue lives of 7000 cycles; (b) stress levels correspond to fatigue lives of 850 000 cycles.

mode up to its failure. A push-pull stress range of 960 MPa and a torsion shear stress level of 580 MPa were selected in low-cycle fatigue (lifetime of 7000 cycles). In high-cycle fatigue a push-pull stress level of 590 MPa and a torsion shear stress level of 380 MPa were chosen (lifetime of 850 000 cycles).

The cumulated cycling results are presented in Fig. 8 for both low and high-cycle fatigue. It is observed that a prior torsional fatigue is more detrimental than a prior push-pull fatigue. This is explained by the cracking directions developed during a first torsion loading sequence. One cracking direction in

torsion (the transversal one) corresponds to stage II cracking direction under push-pull. Hence stage I cracking in push-pull is by-passed as soon as the first cracks are initiated in torsion.

When conducting the opposite sequence the prior push-pull induced cracking is oriented at 45° (with reference to the specimen axis) during stage I cracking. Some of the cracks develop transversely across the bulk during stage II cracking.

As long as the stage II has not been attained during prior push-pull cycling, the push-pull fatigue damage is unable to lower the residual fatigue life under torsion. On the contrary the torsion fatigue life is improved. Push-pull short cracks become dormant during the second sequence of torsion fatigue. This must be related to the change of the stress state.

New short cracks are necessarily initiated under a second torsion fatigue sequence. These cracks are impeded by typical obstacles such as ferrite/pearlite interfaces. Furthermore, dormant push-pull cracks must behave as new supplementary obstacles. The aspect ratio is quite different between push-pull short cracks and torsion short cracks. As a matter of fact push-pull short cracks are on average five times deeper than torsion short cracks. The development path of torsion short cracks is therefore much more influenced by prior push-pull damage than for the opposite situation.

As soon as push-pull short cracks propagate in tensile mode during the first sequence, they are still active and they grow on during the next torsion sequence. The maximum fatigue life increase corresponds to the period of cycles during which the propagation of some short cracks changes over from shear mode (45° oriented in reference to specimen axis) to tensile mode (transversal cracking direction).

Previous work (7) has been performed on the medium carbon steel, in sequential multiaxial fatigue in high-cycle fatigue (400 000 cycles). According to the related results a mean short-crack surface length of 85 μm corresponds to the change of cracking mode. A maximum of the fatigue life increase in torsion was obtained for a first sequence fraction of reduced life under push-pull corresponding to the formation of cracks longer than 85 μm at the surface.

Fatigue life increase is much less in low-cycle fatigue due to the high values of attained stress levels. Furthermore among the many cracks initiated during the first sequence there are always a few which are favourably oriented. Their favoured orientation gives way to continuous development during the following sequence.

7 Conclusion

The fatigue damage in a medium carbon steel accumulates in the same way when comparing different stressing conditions. The comparison of single-phase and ferrite/pearlite material points out the similarity of push-pull fatigue damage accumulation. The existence of different phases simply creates interfaces between the phases, each one being different in its strength to hinder crack propagation.

The similarity of the damage processes between the single phase and the ferrite/pearlite steels can be related to the homogeneity of the distribution of the propagation obstacles, regardless of their nature (either grain boundaries or phase interfaces). As a matter of fact the statistical description of damage deduced from the observations is based on a converging behaviour of individual damage events. The difference between torsion and push-pull fatigue damage only lies in the surface short-crack densities. On average, twice more cracks were numbered under torsion. Finally the residual fatigue life in torsion cycling is strongly influenced by the surface length of short cracks developed under push-pull.

Acknowledgements

The authors would like to thank Professor K. J. Miller whose stimulation and encouragement helped to carry out this study at SIRIUS, Structural Integrity Research Institute, University of Sheffield.

References

(1) MUGHRABI, H. and ACKERMANN, F. (1979) Persistant slip bands in cyclically deformed copper crystals, *ASTM STP*, **675**, ASTM, pp. 69–105.
(2) KITAGAWA, K. and TAKAHASHI, S. (1976) Applicability of fracture mechanics to very small cracks in the early stage, *Int. Conf. Behaviour of Materials, ICM 2*, Boston, 627–631.
(3) WEISS, J. and PINEAU, A. (1993) Continuous and sequential multiaxial low-cycle fatigue damage in 316 stainless steel, *ASTM STP*, **1191**, ASTM, San Diego, 183–192.
(4) MILLER, K. J. (1991) Metal fatigue – past, current and future, Twenty-seventh John Player Lecture, Institution of Mech. Engs., London.
(5) MAGNIN, T., COUDREUSE, L. and LARDON, J. M. (1985) A quantitative approach to fatigue damage evolution in FCC and BCC stainless steels, *Scripta Met.*, **19**, 1487–1490.
(6) BATAILLE, A. and MAGNIN, T. (1994) Surface damage accumulation in low-cycle fatigue: physical analysis and numerical modelling, *Acta Metall. Mater.*, **42**, 3817–3825.
(7) ZHANG, W. (1991) Short fatigue crack behaviour under different loading systems, PhD Thesis, University of Sheffield, U.K.
(8) BATAILLE, A. (1992) Modélisation numérique de l'endommagement physique en fatigue: cas de l'acier 316L et d'un acier ferrito-perlitique, PhD Thesis, University of Lille, France.
(9) MILLER, K. J. (1982) The short crack problem, *Fatigue Fracture Engng Mater Structures*, **5**, 223–232.
(10) BROWN, M. W. (1992) Private discussion.